Spatiotemporal Changes in the Built Environment Characteristics and Urban Heat Island Effect in a Medium-Sized City, Chiayi City, Taiwan

Jou-Man Huang [1],*, Heui-Yung Chang [2] and Yu-Su Wang [2]

[1] Department of Landscape Architecture, National Chiayi University, Chiayi City 60004, Taiwan
[2] Department of Civil and Environmental Engineering, National Kaohsiung University,
     Kaohsiung City 81148, Taiwan; hychang@nuk.edu.tw (H.-Y.C.); yusu84466@gmail.com (Y.-S.W.)
* Correspondence: jouman@mail.ncyu.edu.tw; Tel.: +886-5-2717582

check for
updates

Abstract: This study took Chiayi City—a tropical, medium-sized city—as an example to investigate the urban heat island (UHI) effect using mobile transects and built environment characteristics in 2018. The findings were compared to those from a study in 1999 to explore the spatiotemporal changes in the built environment characteristics and UHI phenomenon. The result for the UHI intensity (UHII) during the day was approximately 4.1 °C and at midnight was approximately 2.5 °C. Compared with the survey in 1999, the UHII during the day increased by approximately 1.3 °C, and the UHII at midnight decreased by approximately 1.2 °C. The trend of the spatial distribution of the increasing artificial area ratio (AAR) proved the importance of urban land use expansion on UHI. The results of the air temperature survey were incorporated with the nesting space in GIS to explore the role of built environment characteristics in UHI effects. The higher the population density (PD) and artificial area ratio (AAR) were, the closer the proximity was to the downtown area. The green area ratio (GAR) was less than 0.2 in the downtown area and increased closer to the rural areas. The built environment factors were analyzed in detail and correlated with the UHI effect. The air temperature in the daytime increased with the population density (PD) and artificial area ratio (AAR), but decreased with the green area ratio (GAR) (r = ±0.3–0.4). The result showed good agreement with previous studies.

Keywords: built environment factors; UHI; tropical medium-sized city; artificial area; building coverage rate; green coverage rate; mobile transects

1. Introduction

Rapid social and economic growth and prosperity have affected the urban thermal environment and caused changes in the local climate, environment, and quality of life of residents. The most obvious issue is the urban heat island (UHI) effect. UHI is defined as a phenomenon in which air temperatures of urban areas are higher than those of the surrounding or rural areas [1]. The urban heat island intensity (UHII), which is the maximum temperature difference between the urban and rural areas, is usually used to measure the severity of UHI [2].

Early studies have found that UHII was related to the size of the city, as indicated by the population [3]. Therefore, many of the UHI research areas have mostly been in large metropolitan areas [4–7]. However, more recent studies have pointed out that the population is only an indicator of the energy exchange between the urban structure and UHI, and the physical form or characteristics of the city are more important for the urban energy balance [8,9]. The effects were investigated of urban development in a tropical area on urban sprawl, the urban heat island (UHI) effect, and metropolitan weather phenomena that are related to the quality of urban life in the Hanoi metropolitan area in

Vietnam. The results imply that during the study period from 1999 to 2016, urban development and its environmental effects have imposed pressing issues and new challenges for sustainable development [10]. From the 2000–2015 Bangkok survey, it was found that urban physical characteristics have a significant impact on the UHI magnitude, particularly the floor area ratio (FAR) and building coverage ratio (BCR), in which temperature levels at 10 p.m. and the thermal cooling rate between 4 and 10 p.m. had a correlation value (r) of over 0.50 [11]. Quite recently, the mobile measurement of the Shenzhen Overseas Chinese Town was incorporated with the GIS-based spatial interpolation and led to a quantified evaluation of the local UHI densities. The spatial distribution results demonstrated that decreasing the building density may help relieve local-scale UHI effects [12]. In addition, according to the 2009 survey in Taichung City, Taiwan, it was found that the street air temperature is correlated with the height-to-width ratio (H/W ratio) (r = 0.481), green ratio (r = 0.729), and BCR (r = 0.654), during the night [13]. In the city of Bogotá, Colombia, the relationship between the UHI and population size was studied while considering population density and urban form parameters of different neighborhoods. The results show that a density of greater than 14,500 inhabitants/km^2 may cause air temperature differences of more than 1 °C, greater obstruction of the sky (SVF < 0.45), and a larger decrease in green areas and vegetation cover (previous surface fraction < 30%) [9].

On the other hand, the basis for economic competitiveness has shifted to the knowledge-based processes of innovation and creativity [14]. The distributions of city sizes, therefore, have not remained the same over time. The UHI effects have also changed with time and space. Medium-sized cities have populations of between 100,000 and 300,000 people [15]. Recently, because the diversity of the commercial activities and manufacturing industries has caused changes in medium-sized cities, there appears to be a renewed interest in the development of medium-sized cities. In the mid-latitude, inland plains of Italy, and the low-latitude coastal plains of Malaysia, researchers have begun to conduct UHI surveys on the medium-sized cities of Padua [16] and Muar [17], where the populations are approximately 150,000–300,000, and have found that the UHII can reach 4–6 °C. Those UHIIs have been almost equal to those of the mega-cities with populations of more than one million, implying that urban characteristics or other factors, such as geographical conditions [4,18], have more important impacts on the UHI. However, there is little research in the medium-sized cities, and the related phenomena and mechanisms still need to be investigated. In addition, medium-sized cities are also in the early stages of development in large cities. Due to the limitations of time, it is difficult to study the UHI in large cities and to trace it back to past urban development. Therefore, if we can understand the more relationship between the heat UHI and the factors of urban building in developing medium-sized cities, we can increase the understanding of the impact of urban expansion on the UHI.

Therefore, this study takes a tropical, medium-sized city, Chiayi City as an example to investigate the UHI and the built environment characteristics in 2018 and compared it with a study conducted in 1999, to explore the spatiotemporal changes in the built environment characteristics and urban heat island (UHI) phenomenon.

2. Materials and Methods

2.1. Measurement of UHI Intensity

This study measured the effects of the UHI using the mobile transect observation method. Mobile measurement is usually carried out using the temperature sensors installed on a car or a mobile platform, using a preplanned route and locations to obtain instant data of the urban temperature. The advantages of the method include the high mobility and the high degree of freedom in the investigation times and places. The disadvantages are the lack of time synchronization and the susceptibility to traffic jams. Therefore, if the method can shorten the observation time and correct for time synchronization and standardization, more accurate results will be obtained.

2.1.1. Study Scope and Measurement Points

The present study took Chiayi City, Taiwan, with a population of approximately 270,000 people, as the research object. It is approximately 31 km from the city to the coastline. Figure 1 shows the survey area, routes, and measurement points. In detail, the survey area was divided into three parts by the routes, i.e., the western, northern, and southern routes. The intersections on the main roads were selected as the measurement points. Moreover, the points were denser in the urban areas and sparser in the rural areas. Each route had approximately 30 measurement points, and there was a total of 87 measurement points. The survey for the three routes was carried out at the same time and completed in 1 h.
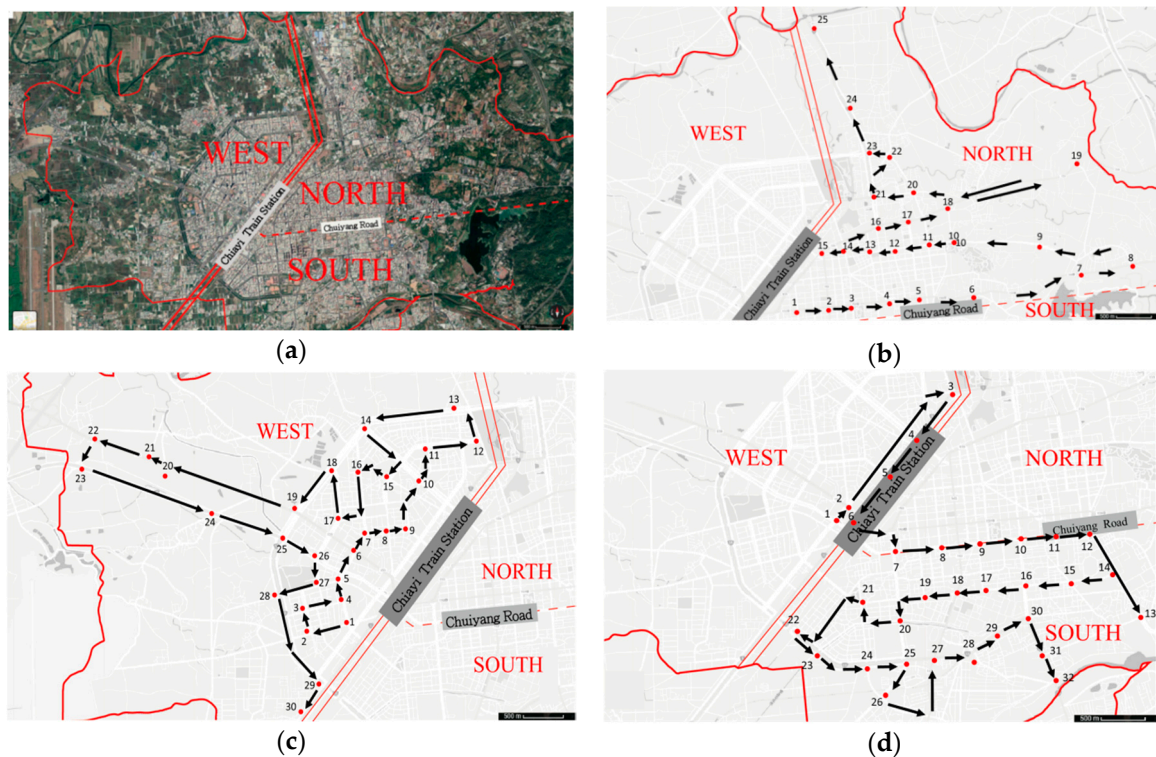
Figure 1. Survey area, three routes, and the locations of 87 measurement points. (**a**) Survey area. (**b**) Northern route and measurement points. (**c**) Western route and measurement points. (**d**) Southern route and measurement points.

2.1.2. Survey Time, Method and Measuring Instruments

The survey was conducted on sunny summer days without rain from 28 July to 31 July 2018. The survey hours were from 10:30 a.m. to 2:30 p.m. and 11:00 p.m. to 2:00 a.m. The measurements were conducted on an hourly basis. The method was to move to the measuring point in a sequence with a group of two people and one motorcycle and stay for 15 s at the measuring point, recording one data point every 2 s. The time synchronization of the measurements and recording devices was performed before the survey to ensure that each route remained synchronized.

The measurement and recording device used was the outdoor temperature and humidity recorder HOBO MX2301 (Onset co.), which has a temperature measurement range of −40 °C to 70 °C with an accuracy of ±0.2 °C. The data were also collected and recorded every 5 min in the fixed weather station in Lantan Campus, National Chiayi University, to correct for the time synchronization. The device used in the weather station was the HOBO RX3000 (Onset co.), which has a temperature measurement accuracy of ±0.2 °C.

2.1.3. Correction for Time Synchronization

For each hourly observation, the data recorded at the midpoint of the time period were used as the reference for the correction. For example, an hourly observation was made for the time period from 1:00 to 2:00, and the mid-time point was 1:30. As mentioned, the data were collected and recorded every 5 min at the weather station, and the data were measured and recorded every 2 min along the survey routes. These data were corrected within a period of 2 min. For example, if the weather station collected data at 10:32 and 10:37, and the survey measured data at 10:34, then the 10:32 data from the weather station should be used to correct the 10:34 survey data for time synchronization. The range of the time correction was approximately ±0.2–0.9 °C, with an average of −0.06 °C.

2.1.4. Background Weather Conditions

The UHI phenomena are more easily observed when the weather phenomena on large scales are weak, or on sunny summer days with no rain. Table 1 summarizes the background weather conditions during the survey. To facilitate the comparison with the 1999 study, the background weather conditions of the survey day in 1999 are also compiled in Table 1. The weather data were from the Chiayi weather station, Taiwan Central Weather Bureau [19]. After comparing the hourly temperature data, during the daytime measurement period on 29 July, the cloud volume was the lowest that had been observed, the wind speed was low, and the temperature was high, making it the most representative day during the observation period.

Table 1. Background weather conditions during the survey.

Parameter	28 July 2018					29 July 2018				
	10	11	12	13	14	10	11	12	13	14
Temperature (°C)	32.3	32.5	33.8	34.0	34.0	33.0	33.5	34.1	35.0	34.8
Wind velocity (m/s)	2.1	0.9	1.1	2.0	3.1	1.4	1.3	2.5	1.6	4.6
Cloud cover (0–10)	6	8	7	7	7	3	3	3	3	6
Radiation (MJ/m^2)	2.21	1.90	1.82	2.43	2.49	2.51	3.00	3.02	3.32	2.52
Rainfall (mm)	0.0	0.0	0.0	0.0	0.0	0.0	0.0	0.0	0.0	0.0

Parameter	30 July 2018					30 July 2018		31 July 2018	
	10	11	12	13	14	23	24	1	2
Temperature (°C)	32.8	33.1	33.5	34.7	34.7	28.7	28.4	28.1	27.1
Wind velocity (m/s)	0.8	3.0	1.7	3.7	4.2	1.1	0.7	0.9	0.4
Cloud cover (0–10)	4	4	6	2	2	–	–	–	–
Radiation (MJ/ m^2)	2.66	2.73	2.32	3.11	3.00	0.0	0.0	0.0	0.0
Rainfall (mm)	0.0	0.0	0.0	0.0	0.0	0.0	0.0	0.0	0.0

Parameter	16 August 1999					16 August 1999		17 August 1999	
	10	11	12	13	14	23	24	1	2
Temperature (°C)	30	30.7	31.1	31.5	31.5	27.1	26.6	26.5	25.2
Wind velocity (m/s)	2.7	2.3	2.8	3.9	3.7	0.7	0.3	0.9	0.3
Cloud cover (0–10)	–	4	–	–	3	0	–	–	0
Radiation (MJ/m^2)	1.70	2.34	2.34	2.23	1.87	0.0	0.0	0.0	0.0
Rainfall (mm)	0.0	0.0	0.0	0.0	0.0	0.0	0.0	0.0	0.0

2.2. Analysis of the Built Environment Factors

Previous studies [8–11] have shown that built environment factors or urban physical characteristics such as population density, building cover ratio, floor area ratio, and anthropogenic heat, can significantly affect the UHI intensity. The population density can show the concentration and distribution of the urban population and the urbanization intensity within a city [9] and be used as a metric to determine spatial variation in electrical use and thus estimate energy consumption

and the magnitude of anthropogenic heat in a city [9,20]. Urban land cover, such as building cover, green coverage, water surface, and street surface ratios [8,9,11], is related to urban land use and alters the urban energy balance [9,21]. Therefore, this study first analyzed the district-scale population density (PD), artificial coverage ratio (AAR), and green coverage ratio (GAR) to investigate their roles in UHI formation. In detail, data were first collected from the district population and areas from the 2018 official website [22], and then ratios were used to obtain the population density for each district. Aerial photographs from 2014 [23] were then collected for Chiayi City and used to analyze the artificial coverage and green coverage ratios for each district. The AAR describes the proportion of the urban land cover plan area occupied by artificial objects (built-up and street areas), and GAR describes the proportion of the urban land cover plan area occupied by plants (park and green areas). We also analyzed the 100-m building coverage ratio (BCR, built-up area) and investigated its role in UHI formation. In greater detail, the building area and the coverage ratio were calculated for the area enclosed by a circle with a 100-m diameter with the center located in each survey point. These district-scales and 100 m-scale built environment factors aided in obtaining a better understanding of UHI effects and spatial changes.

2.3. Correlation Analysis

For understanding the correlation between the air temperature and each built environment factor, linear regression analysis was performed and yielded the coefficient of relevance (r) as a reference indicator for discussion. In addition, to facilitate an understanding of the results of r for discussion and comparison, we referred to the results of the study in 1999 [24,25] and statistical definitions to define the magnitude of correlation as of the following three types. If the r was equal to or greater than 0.50, the factor was considered to be highly correlated with the UHI. If the r ranged from 0.3 to 0.5, the factor was considered to be moderately correlated with the UHI. If the r was less than 0.30, the factor was considered to be weakly correlated with the UHI.

3. Results and Discussion

Lin et al. [24,25] also completed mobile transect observations in Chiayi City and evaluated the UHI effects in 1999. The survey had three routes, each route had approximately 70 measurement points, and each was carried out at the same time and completed in 1.5 h. The daytime and nighttime measurement periods were from 12:00 to 14:00 and from 2:00 to 4:00, respectively, and the time synchronization point was 14:00 and 2:00, respectively [24,25]. This allowed us to compare these data in detail to those of the present work to understand the spatiotemporal changes in the built environment characteristics and UHI.

3.1. UHI Temperature

3.1.1. Daytime

Figure 2a,b depict the contours of UHI temperature for the summer daytime in Chiayi City in 1999 and 2018. The 1999 survey obtained the highest temperature of 33.9 °C near the central area and the lowest temperature of 31.1 °C near the Lantan Reservoir area. The 2018 survey obtained the highest temperature of 37.5 °C and the lowest temperature of 33.4 °C (the average of 28 and 29 July). Accordingly, both surveys had a low-temperature zone near the Lantan Reservoir. During the last two decades, the daytime variation of the highest temperature increased by approximately 3.5 °C, the daytime variation in the lowest temperature increased by approximately 2.5 °C, and the daytime UHII increased from 2.8 °C to 4.1 °C in Chiayi City. Furthermore, in the spatial distribution of the high-temperature regions, it can be found that the high-temperature regions in 2018 had a tendency to expand to the east, west, northwest, and south compared with the results of the 1999 survey, and in the changes of the low-temperature regions, there was a tendency to concentrate on the west areas.

Compared to the similar medium-sized city, the population with approximately 150,000–200,000 people, Padua, Italy, and Muar, Malaysia, [16,17] it can be found that the UHII in the mid-latitude, inland cities of Padua, Italy, was 2.0 °C higher than that in Chiayi City. The UHII in the tropical, coastal city of Muar, Malaysia, was equal to that in Chiayi City. The results of this study were consistent with the previous research and imply that even if the city size is similar (population), the difference in latitude or geographic location of the city would have a certain degree of influence on the strength of the UHIs.
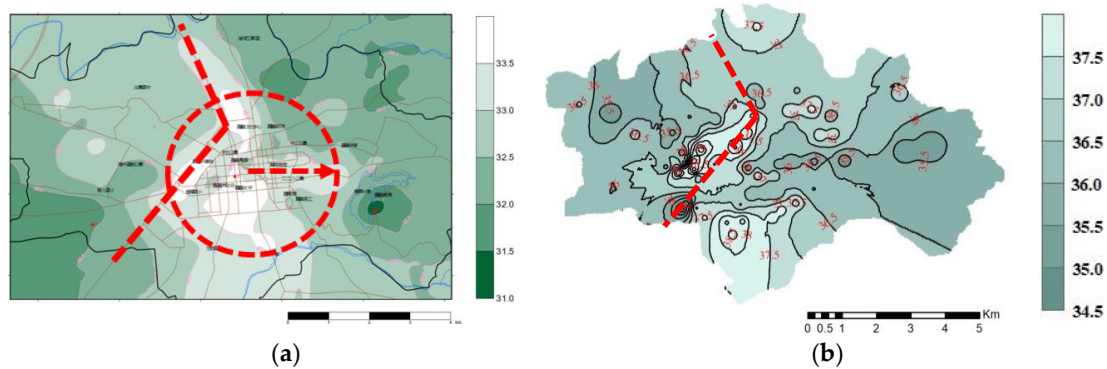
Figure 2. Spatial changes in the daytime UHI temperature from 1999 to 2018; (**a**) 16 August 1999 2:00 p.m. [25]; (**b**) 29 July 2018 2:00 p.m. (the present study).

3.1.2. Midnight

Figure 3a,b depict the contours of UHI temperature for the summer midnight in Chiayi City in 1999 and 2018. The 1999 survey gave the highest temperature of 27.6 °C and the lowest temperature of 23.9 °C. The 2018 survey gave the highest temperature of 28.5 °C and the lowest temperature of 26.0 °C. During the last two decades, the highest temperature increased by approximately 1.1 °C, the lowest temperature increased by approximately 2.1 °C, and the midnight UHII decreased from 3.7 °C to 2.5 °C in Chiayi City. The decrease in the night UHII may be due to the land use expansion in the outer portion of the center area and the eastern suburbs, which results in a decrease in the nighttime air temperature of the suburbs, where the night cooling effect should be strong, which resulted in a smaller difference from the highest temperature. In addition, the spatial distribution of the high-temperature regions was similar to that in 1999, but there was a trend of expansion to the northwest and southwest. The distribution of the low-temperature regions was also similar to that in 1999, but the original cold zone of the north and southwest side had a tendency to decrease towards the western side.
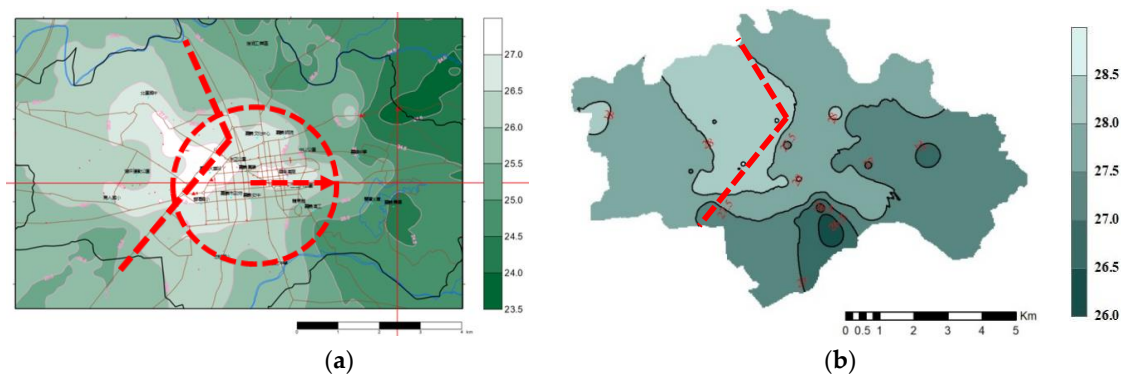
Figure 3. Spatial changes of the midnight UHI temperature from 1999 to 2018. (**a**) 17 August 1999 2:00 a.m. [25]; (**b**) 31 July 2018 1:30 a.m. (the present study).

3.1.3. Changes in the Artificial Area Ratio from 20 Years Ago vs. UHI

The study collected, analyzed, and compared the 2005 and 2014 aerial photos to calculate the area of the built environment and the coverage ratio (i.e., artificial area ratio). This broadens the understanding of the expansion of the commercial and industrial activities in Chiayi City during the last two decades. Figure 4 shows the increase rate for each district. It was found that in the central area, the increase rate ranged between 0% and 30% (approximately 2 km radius around the Chiayi Railway Station, C1), and the increase appeared to be trivial. For the zone between the central and rural areas, the subcentral areas (approximately 2–4 km radius around the Chiayi Railway Station, C2), the ratios of increase changed from 45% to 90% or higher, and this increase appeared to be the highest one. In the rural area, approximately 2–4 km from the subcentral area (C3–C4), the increase again dropped to 30% and below.

Moreover, in the subcentral area with the highest increase, the northeast, east, northwest, west, and southwest sides had the most obvious increase ratios. The spatial change trend of increasing the artificial area ratio was consistent with the trend of the UHI between 2004 and 2015 (Figures 2 and 3) and distinctly indicated the importance of the influence of urban land use expansion on the UHIs.
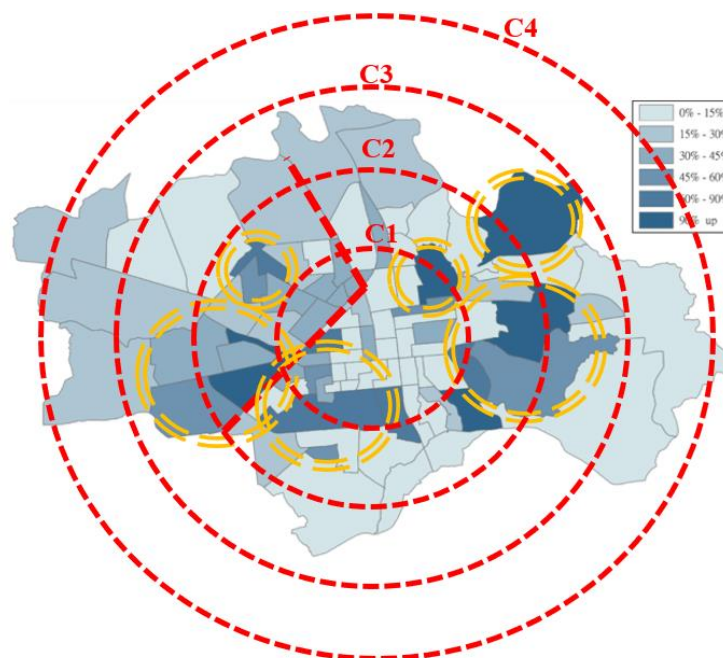
Figure 4. Increase rates of artificial areas between 2005 and 2014.

3.1.4. Influence of Climate Change in 1999 and 2018

Many studies have shown that climate change has led to an increase in the air temperature. To understand how much the UHI results between 1999 and 2018 survey may have been affected by climate change, we further collected and analyzed data. The results found that according to the IPCC survey report, the global air temperature increased by approximately 0.85 °C during the past 100 years (1880–2012), while it increased by approximately 1.3 °C in Taiwan (1900–2012) [26]. This change translates into an annual average air temperature increase rate of 0.006 °C/year and 0.012 °C/year, respectively. According to these data, the air temperature increases, which may have been affected by global warming from 1999 to 2018, were approximately 0.11 °C and 0.23 °C, respectively. If the UHI results for 1999 and 2018 are deducted by the values that may be a result of global climate change, the air temperature increase over the past 20 years remains significantly greater than the global warming effect (Table 3). This result also indicates that in comparison to the global warming effect, the UHI effect affected by urbanization is more serious and important.

3.1.5. Influence of Measurement Difference in 1999 and 2018

Table 2 lists a comparison of the UHI measuring differences between the studies of 1999 and 2018 and indicates that the differences are mainly terms of the (A) measuring method and (B) measuring time. Differences in the (A) measuring method could result in problems of measuring accuracy. The 2018 survey (the present study) has a higher accuracy for instrument measurement and per-route measuring period. Although the measuring points are fewer than in 1999 and the accuracy may be lower, the total results could be mutually offset. As a result, the difference in the accuracy is small and can be ignored. The difference in measuring time mainly results in a difference in background weather conditions (B1) and the problem of air temperature change caused by an inconsistent measuring period (B2, B3). During the day, while the measuring period of 2018 was 1–1.5 h later than that of 1999, the two were corrected to become the same time point (14:00) and can be regarded as consistent. During the midnight measuring period, there was a similar situation. After time synchronization, although the 2018 survey remained 0.5 h earlier than 1999 survey, via comparison of the data from the weather station (for correction), the air temperature difference between 1:30–2:00 was only approximately ±0.03–0.2 °C. Therefore, the main error resulting from the difference in the measuring methods was the difference in the background weather condition caused by the inconsistent measuring date (B1).

According to Table 1, the main difference in the background weather conditions during the 1999 and 2018 surveys was the effects of solar radiation (global solar radiation) on air temperature. During the day, the average hourly radiation on 16 August of 1999 and 28 and 29 July of 2018 was 1.32, 1.51 and 1.80 MJ/m^2 respectively (Table 3). Thus, the radiation during the 2018 survey was higher by 15% (28 July) and 32% (29 July) than during 1999. To analyze the air temperature increase caused by the higher radiation in 2018, we further used the meteorological data of the Taiwan Central Weather Bureau [19] to analyze the values of air temperature increase caused by radiation variation. We assumed that the air temperature increase from 1999 to 2018 was mainly due to three effects: (1) global warming, (2) the UHI effect, and (3) the effect of higher radiation on measuring days of 2018. The effect of global warming (1) is as described in Section 3.1.4, and the UHI effect (2) is the air temperature variation caused by urban expansion, land use change, human activities, etc. The discussion of the air temperature increase caused by radiation variation (3) must select the time point that was not affected by changes in urban development during 1999 and 2018, and the date in which other background weather conditions were consistent with the baseline date. Therefore, with 8/16 of 1999 as the reference date and using the global solar radiation (X) and air temperature (Y) from 6:00 to 18:00, a linear regression equation was obtained: $y = 2.5253x + 26.053$ of $R^2 = 0.75$ (interpretation of 75%). Accordingly, substituting the values of global solar radiation on 28 July and 29 July of 2018, and estimating the air temperature increase only caused by the radiation variation, the results showed that the average air temperature difference (13:00–15:00) was +0.60 and +1.33 °C, respectively, with the average of these as +0.97 °C. At midnight, because the air temperature was affected by radiation during the day, the analysis was conducted in the same manner. Substituting the values of global solar radiation on 30 July of 2018, the results showed an average air temperature difference of +1.22 °C (6:00–18:00).

In addition, the effects of the air temperature increase via (1) global warming, and (3) the radiation variation of the measuring date compared to 1999 mainly affected the difference between the highest and the lowest temperature during the 20 years for the day and midnight. The results are summarized and listed in Table 3.

Table 2. Comparison of the UHI measuring differences between the 1999 and 2018 studies.

Year	(A) Measuring Method			(B) Measuring Time			
	Measuring Accuracy (A1)	Measuring Points (A2)	Measuring Period of Each Route (A3)		Date (Radiation (MJ/m^2)) (B1)	Period (B2)	Correction Point (B3)
1999	±0.5	208	1.5 h	Daytime	16 August (1.32)	12:00–14:00	14:00
				Midnight	August 17 (1.32)	2:00–4:00	2:00
2018	±0.2	87	1 h	Daytime	July 28 (1.51) July 29 (1.80)	13:30–14:30	14:00
				Midnight	July 31 (1.80)	1:00–2:00	1:30

Table 3. Summary of the UHI temperature difference between 1999 and 2018.

UHI Difference between 1999 and 2018 (°C)			(A) Consideration of Climate Change Effects		(B) Consideration of the Solar Radiation Difference	Consideration of (A) + (B)	
			Deducting Global Warming (A1)	Deducting Global Warming in Taiwan (A2)		(A1) + B	(A2) + B
Period/Values			(−0.11)	(−0.23)	(Daytime: −0.97 Midnight: −1.22)		
Daytime	ΔT_{max}	+3.5	+3.39	+3.27	+2.53	+2.42	+2.30
	ΔT_{min}	+2.5	+2.39	+2.27	+1.53	+1.42	+1.30
Midnight	ΔT_{max}	+1.1	+0.99	+0.87	−0.12	−0.23	−0.35
	ΔT_{min}	+2.1	+1.99	+1.87	+0.88	+0.77	+0.65

3.2. Built Environment Factors in Chiayi City

3.2.1. Population Density (PD)

The PD in Chiayi City averaged approximately 1000 people/km^2. Figure 5a,b give the frequency and spatial distribution of the PD by city districts. Figure 5a indicates that 91% of the districts had a population density of 0–1800 people/km^2, and 8.4% of the districts had a PD greater than 1800 people/km^2. Figure 5b shows the spatial distribution of the PD. It appears that for the districts near the central train station area, the values were higher and showed more than 900 people/km^2, but for the districts near the rural areas, the values were smaller and showed less than 600 people/km^2. In other words, the population density increased when approaching the station. The population density decreased by moving away from the station.
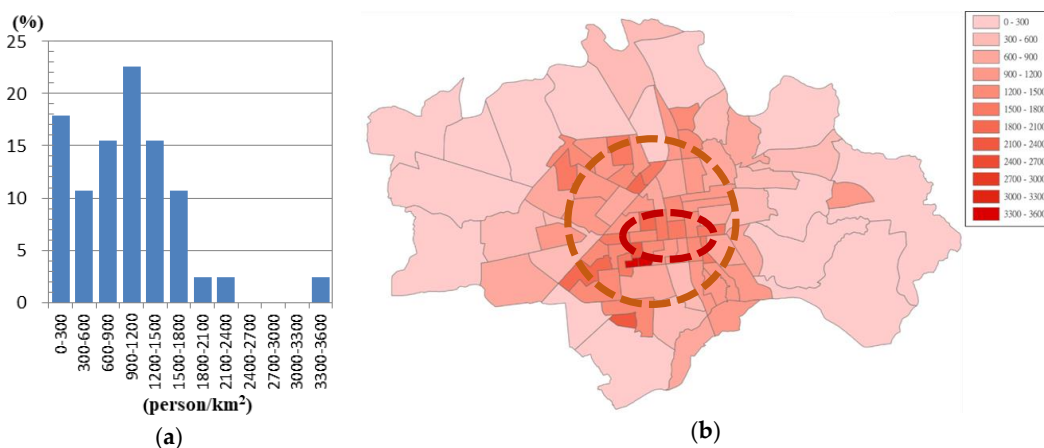
Figure 5. Distribution of population density by city districts. (**a**) Frequency distribution; (**b**) Spatial distribution.

3.2.2. Green Area Ratio (GAR)

Figure 6 shows the green area ratio (GAR) and the frequency distribution for each district in Chiayi City. The ratio was lower than 0.4 for the majority of the city (approximately 71% of the districts). The ratio decreased to 0.2 and lower in the areas located approximately 2.0 km from the train station or city center. The further away from the city center, the greater the GAR. The distribution of the GAR in Figure 6 had an opposite trend when compared to that of the artificial area ratio (AAR) in Figure 7. The ratio was higher than 0.8 for a minor part of the city (nearly 10% of the districts). The ratio was greater than 0.6 for the districts near the Lantana Reservoirs and the newly constructed high-speed railway station.
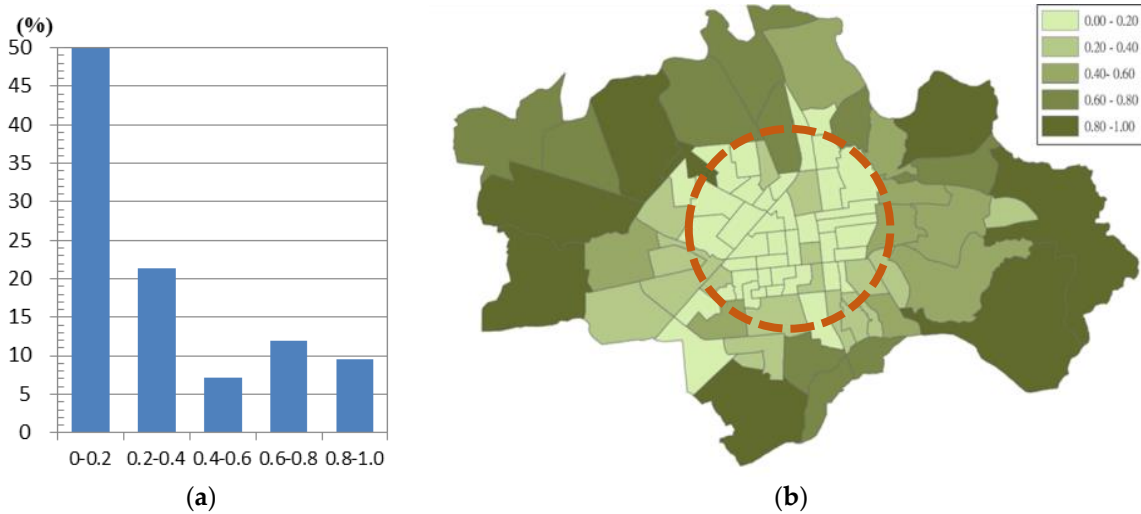
Figure 6. Distribution of the green coverage ratio by city districts. (**a**) Frequency distribution; (**b**) Spatial distribution.

Figure 7. *Cont.*

(**c**)
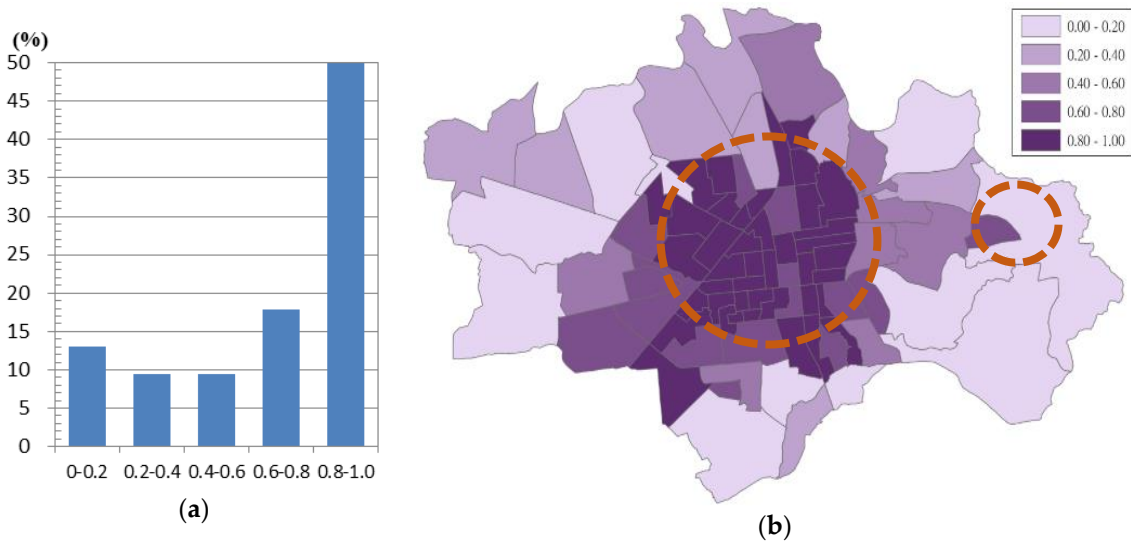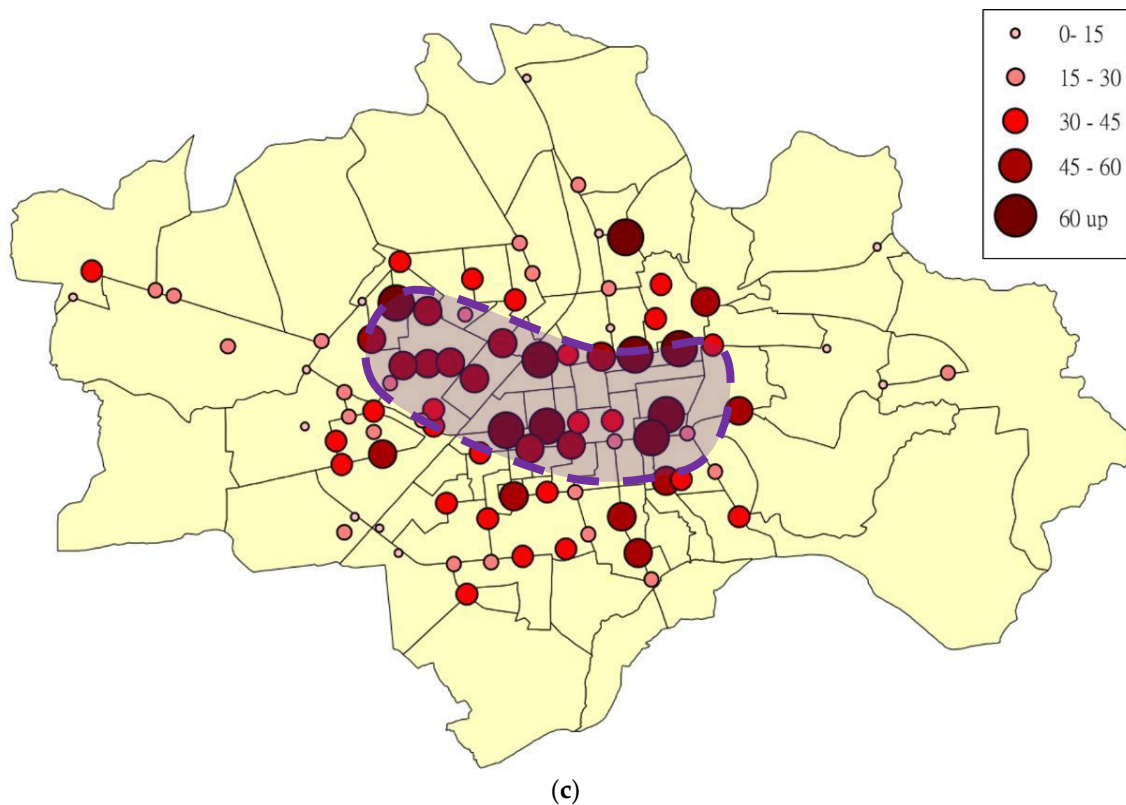
Figure 7. Distribution of the artificial area ratio. (**a**) District-scale frequency distribution; (**b**) District-scale spatial distribution; (**c**) 100 m-scale for each survey point spatial distribution (the building area ratio).

3.2.3. Artificial Area Ratio (AAR)

Figure 7 shows the artificial area ratio (AAR) for each district. In detail, the building area or coverage ratio was calculated for the area enclosed by a circle with a 100-m diameter with the center located in each survey point. Figure 7a showed that approximately 50% of the districts had a value between 0.8 and 1.0, followed by 18% of the districts, and the districts with values between 0.6 and 0.8 and lower than 0.4 were less than 23% of all districts. Figure 7b shows the spatial distribution of the AAR. The results showed that the AAR more than 0.6 was mostly concentrated in the area with a radius of approximately 3 km around the railway station. The values were all less than 0.4 for the Lantan District in the rural area on the east side (except the Daya Road shopping district), as well as in the North Port Road and the high-speed rail area on the west side.

These 100 m-scale building area ratios (BAR) and the effects were analyzed and compared to the district-scale ratios to gain a better understanding of the UHI formation and the spatial changes. The results are shown in Figure 7c and appear to show that in the central area (near railway station), the values could reach 60 and were obviously higher than for other parts of the districts.

3.3. Coefficient of Correlation between the UHI and Built Environment Factors

3.3.1. District-Scale Analysis

Table 4 provides an example of the linear regression analysis of the UHI temperature and district-scale built environment factors. The correlation coefficient(r) not only changed for the built environment factors but also varied significantly according to the survey time. As expected, the UHI temperature increased with population density and artificial coverage ratio but decreased with the green coverage ratio. As illustrated by the table, district-scale built environment factors, such as the population density, artificial area ratio, and green coverage ratio moderately related with the air

temperature surveyed at 1:00 p.m. (r > 0.3), and this trend was more obvious at 2:00 p.m. (r > 0.4, except PD).

Table 4. Results of linear regression analysis on 28 June 2019 daytime UHI temperature and the district-scale built environment factors (N = 84).

Time	A.M. 11:00	12:00	P.M. 1:00	2:00
Population density	$y = -9 \times 10^{-5}x + 34.714$ r = −0.10	$y = -6 \times 10^{-5}x + 36.112$ r = −0.10	y = 0.0004x + 35.129 **r = 0.36**	y = 0.0003x + 34.951 **r = 0.28**
	weak correlation	weak correlation	moderate correlation	weak correlation
Artificial area ratio	y = 0.4412x + 34.318 r =0.13	y =0.2061x+ 35.9075 r = 0.08	y =0.9253x + 34.851 **r = 0.34**	y = 1.3886x + 34.33 **r = 0.42**
	weak correlation	weak correlation	moderate correlation	moderate correlation
Green area ratio	y = −0.4438x + 34.76 r = −0.10	y =−0.2117x + 36.115 r = −0.10	y =−0.9221x + 35.775 **r = −0.35**	y = −1.3876x + 35.719 **r = −0.41**
	weak correlation	weak correlation	moderate correlation	moderate correlation

3.3.2. 100 m-Scale Analysis

Table 5 summarizes the results of the linear regression analysis on the UHI temperature and 100 m-scale building coverage ratio. For the overall Chiayi City area, the district-scale artificial area ratio had the greatest r of 0.42 for the temperature surveyed at 2:00 p.m., and the 100 m-scale building coverage ratio also had the greatest r of 0.42 for the temperature surveyed at 1:00 p.m. (see Tables 4 and 5). These two factors were thought to have very similar effects on the UHI and gave the same coefficient of correlation with the surveyed temperature.

Table 5. Results of the linear regression analysis on the 28 June 2018 daytime UHI temperature and 100 m-scale building coverage ratio (N = 87).

Time	A.M. 11:00	12:00	P.M. 1:00	2:00
Chiayi City	y = 0.0073x + 34.303 r = 0.14	y = −0.0077x + 36.335 r = −0.17	y = 0.0189x + 34.71 **r = 0.42**	y = 0.0146x + 34.9 r = 0.26
	weak correlation	weak correlation)	moderate correlation	weak correlation
Northern area	y = 0.0092x + 34.642 r = 0.14	y = 0.0025x + 36.033 r = 0.10	y = 0.0096x + 35.349 r = 0.33	y = 0.0152x + 34.703 r = 0.28
	weak correlation	weak correlation	moderate correlation	weak correlation
Southern area	y = 0.0152x + 33.683 r = 0.24	y = 0.0106x + 35.362 r = 0.32	y = 0.019x + 34.681 r = 0.28	y = 0.0262x + 34.341 r = 0.39
	weak correlation	moderate correlation	weak correlation	moderate correlation
Western area	y = −0.0057x + 34.697 r = −0.14	y = −0.0294x + 37.204 r =−0.46	y = 0.023x + 34.402 **r = 0.58**	y = 0.0152x + 35.174 r = 0.30
	weak correlation	moderate correlation	highly correlated	moderate correlation

As illustrated by the table, the UHI temperature increased with the building coverage ratio as expected. Moreover, the coefficients of correlation not only changed for the survey areas but also varied depending on the survey time. In detail, the building coverage ratio highly correlated with the 1:00 p.m. UHI temperature in the western area (r = 0.58 > 0.5), and the correlation was much greater than those at the other survey time and in the other areas.

3.3.3. Time-Scale Analysis

The present study made mobile transect observations in Chiayi City in 2018, analyzed the population density, artificial area ratio, and green coverage ratio, and calculated the coefficients of correlation with the UHI temperatures. Table 4 summarizes the coefficients of the correlation (r) between the built environment factors and the UHI temperatures. The population density and the artificial area ratio affected the UHI daytime temperatures relatively more significantly. In contrast, the green coverage ratio was also affected, and the coefficient of correlation was slightly greater for the UHI midnight temperature.

Lin et al. [24,25] made mobile transect observations in Chiayi City in 1999, analyzed the 1000 m-scale population density, artificial area ratio, and green coverage ratio, and calculated the coefficients of correlation with the UHI temperatures. As illustrated in Table 6, the r has decreased in the last two decades. Specifically, the population density was highly correlated with the UHI daytime temperature in 1999 (r = 0.67 > 0.5), but the correlation became relatively weak in 2018 (r = 0.28 < 0.5). There were similar trends in the other two built environment factors and in the midnight UHI temperatures.

Table 6. The r between UHI temperature and built environment factors in 1999 and 2018.

Time	1999 [24,25]		2018 (the Present Study)	
	Daytime	**Midnight**	**Daytime (2:00 p.m.)**	**Midnight (0:30 a.m.)**
population density	r = 0.67	r = 0.60	r = 0.28	r = 0.27
	highly correlated	highly correlated	moderate correlation	weak correlation
Artificial area ratio	r = 0.63	r = 0.52	r = 0.42	r = 0.27
	highly correlated	highly correlated	moderate correlation	weak correlation
Green area ratio	r = −0.62	r = −0.60	r = −0.41	r = −0.28
	highly correlated	highly correlated	moderate correlation	weak correlation

The reason why the correlation coefficient (r) of this study was lower than the value of 1999 is probably for the different calculation ranges. Lin et al.'s research [24,25] used built environment factors in the range of 1000 m radius from measurement points, while this study mostly used those factors in the range of approximately 200–300 m. The results of the correlation coefficient seem to indicate that the results of the built environment factors with a large radius, such as 1000 m, can better reflect the relationship between the UHI effects obtained by mobile transects and built environment factors. However, according to the analysis results of the smaller range, 100 m-scale, artificial coverage rate in this study, the correlation can be improved to approximately 0.4–0.6 (Table 5). Therefore, in the discussion of the correlation between the urban built environment factors and the UHI effects obtained by the mobile transects, it is useful to select the appropriate extent areas for analysis. In other words, it is an issue worthy of further research to determine how much the UHI effects of the block scale would be affected by the built environment factors within a certain distance.

4. Conclusions

This study took a medium-sized city in the tropics that has rarely been used as a research object, investigated the UHI effect and the built environment factors, and explored their relevance. The results of the study were also compared to those of a previous study in 1999 to discuss the impacts of urban land use expansion on the UHI effect. The present findings contribute to our understanding of the UHI effect in medium-sized cities and indicate new possible study issues for UHIs in future research. The main findings obtained are summarized as follows.

In the UHI survey results in Chiayi City:

(1) The maximum temperature of the UHI in the day was approximately 37.5 °C, and the lowest temperature was approximately 33.5 °C. In comparison with the study in 1999, the maximum temperature difference was approximately +2.3 °C, the minimum temperature difference was approximately +1.3 °C, and the UHII was increased from 2.8 °C to approximately 4.1 °C.

(2) The maximum temperature of the UHI at midnight was approximately 28.5 °C, and the lowest temperature was approximately 26.0 °C. In comparison with the study in 1999, the maximum temperature difference was approximately −0.4 °C, the minimum temperature difference was approximately +0.7 °C, and the UHII was decreased from 3.7 °C to approximately 2.5 °C.

(3) The day-time UHII was consistent with those found in the other medium-sized cities with similar populations of 200,000–300,000 and was comparable to those of large cities with populations of more than one million. Otherwise, it was also found that the UHII of a medium-sized city in the mid-latitude (Padua, Italy) was approximately 2.0 °C higher than those of the medium-sized cities in the tropics (Chiayi, Taiwan and Muar, Malaysia).

(4) According to the analysis of the increase in the artificial coverage ratio between 2004 and 2015, it was found that the increase of the center area was the lowest, while the sub-central area, the outer 2 km radius of the center area, had the highest increase at approximately 45%–90%. Outside of the sub-central area, it again fell to below 30%. In the sub-central area with the highest increase, the northeast, east, northwest, west, and southwest sides had the most obvious increase ratios. This trend was consistent with the trend of the spatial changes in UHI (day-time and night-time) between 2004 and 2015, and it clearly proved the importance of the influence of urban land use expansion on UHIs.

In the results of district-scale built environment factors in Chiayi City:

(1) The population density averaged approximately 1000 persons/km^2, and its spatial distribution had a tendency to decrease outward from the central area (=900 persons/km^2) to rural areas (<600 persons/km^2).

(2) The green coverage ratio averaged approximately 0.32, and in contrast to the population density, its spatial distribution tended to increase outward from the central area (=0.2) to the rural area (>0.6).

(3) The building coverage ratio averaged of approximately 0.66, and its spatial distribution was consistent with the population density, as it tended to decrease outward from the central area (=0.6) to the rural area (<0.4).

In the results of the correlation analysis of the UHI and the built environment factors:

(1) The results indicated that the correlation coefficient(r) between the daytime (1:00–2:00 p.m.) urban temperatures and district-scale (approximately 200–300 m) built environment factors, population density, greening coverage ratio, and artificial coverage ratio were all above 0.3, and the temperature was positively correlated with the population density and artificial coverage ratio and negatively correlated with green coverage ratio. This trend was more obvious in the results of 2:00 pm readings, and the r reached 0.4.

(2) Compared with Lin et al.'s results in 1999, the results of the analysis of the three district-scale built environment factors were consistent, and only the r decreased to 0.3–0.35. This may be due to the different analysis ranges of the built environment factors between the studies (1000 m in Lin et al.'s study, 200–300 m in this study). However, according to the analysis at the smaller scale, the 100 m-scale, artificial coverage ratio in this study, it was found that the r could be increased to 0.4–0.5. Therefore, in future analyses of data from block-scale UHI data obtained through the mobile observation method and built environment factors, the distance range of the built environment factors from measure points should be quantified, and the values could become representative. In other words, the block-scale UHI will be affected by the proximity of built environment factors, which is worthy of further research.

Although in this study, the total number of the population was used to determine city size, other physical (or spatial) factors should be considered as important factors to determine city size, such as population density (person/ha), land use, floor area ratio, and building height. Therefore, these factors are worthy of further research. In addition, these findings provide some insights regarding UHI mitigation. Because the influence of urban land use expansion is important in UHIs, the best way to decrease thermal environment deterioration from the land use expansion process and apply this solution to urban planning policies should be important issues in the development of modern cities, and should be addressed in future studies.

Author Contributions: J.-M.H. and H.-Y.C. made a survey plan and determined the investigation of the scale effects; J.-M.H. and A.-H.W. performed the survey, corrected the temperature data, and integrated it into a GIS; J.-M.H., A.-H.W., and H.-Y.C. analyzed the data; and J.-M.H. and H.-Y.C. wrote the paper. All authors have read and agreed to the published version of the manuscript.

Conflicts of Interest: The authors declare no conflict of interest.

References

1. Oke, T.R. The energetic basis of urban heat island. *J. R. Meteorol. Soc.* **1982**, *108*, 1–24. [CrossRef]
2. Oke, T.R. *Boundary Layer Climates*, 2nd ed.; Methuen & Co.: London, UK, 1987.
3. Oke, T.R. City size and urban heat island. *Atmos. Environ.* **1973**, *7*, 769–779. [CrossRef]
4. Santamouris, M. Analyzing the heat island magnitude and characteristics in one hundred Asian and Australian cities and regions. *Sci. Total Environ.* **2015**, *512*, 582–598. [CrossRef] [PubMed]
5. Giridharan, R.; Rohinton, E. The impact of urban compactness, comfort strategies and energy consumption on tropical urban heat island intensity: A review. *Sustain. Cities Soc.* **2018**, *40*, 677–687. [CrossRef]
6. Chapman, S.; Watson, J.E.; Salazar, A.; Thatcher, M.; McAlpine, C.A. The impact of urbanization and climate change on urban temperatures: A systematic review. *Landsc. Ecol.* **2017**, *32*, 1921–1935. [CrossRef]
7. Tzavali, A.; Paravantis, J.P.; Mihalakakou, G.; Fotiadi, A.; Stigka, E. Urban heat island intensity: A literature review. *Fresenius Environ. Bull.* **2015**, *24*, 4537–4554.
8. Khamchiangta, D.; Dhakal, S. Physical and non-physical factors driving urban heat island: Case of Bangkok Metropolitan Administration, Thailand. *J. Environ. Manag.* **2019**, *248*, 109285. [CrossRef] [PubMed]
9. Ramírez-Aguilar, E.A.; Souza, L.C.L. Urban form and population density: Influences on Urban Heat Island intensities in Bogotá, Colombia. *Urban Clim.* **2019**, *29*, 100497. [CrossRef]
10. Nguyen, T.M.; Lin, T.H.; Chan, H.P. The environmental effects of urban development in Hanoi, Vietnam from satellite and meteorological observations from 1999–2016. *Sustainability* **2019**, *11*, 1768. [CrossRef]
11. Pakarnseree, R.; Chunkao, K.; Bualert, S. Physical characteristics of Bangkok and its urban heat island phenomenon. *Build. Environ.* **2018**, *143*, 561–569. [CrossRef]
12. Liu, L.; Lin, Y.; Wang, L.; Wang, D.; Shiu, T.; Chen, X.; Wu, Q. Analysis of local-scale urban heat island characteristics using an integrated method of mobile measurement and GIS-based spatial interpolation. *Build. Environ.* **2017**, *117*, 191–207. [CrossRef]
13. Sun, C.Y. A street thermal environment study in summer by the mobile transect technique. *Theor. Appl. Climatol.* **2011**, *106*, 433–442. [CrossRef]
14. Spencer, G.M. Economic Development Strategies for Mid-Sized Cities in the Global Knowledge Economy. Available online: https://www.evergreen.ca/downloads/pdfs/2017/14_MSC_RC_Spencer.pdf (accessed on 5 September 2019).
15. Henderson, V. Medium size cities. *Reg. Sci. Urban Econ.* **1997**, *27*, 583–612. [CrossRef]
16. Busato, F.; Lazzarin, R.M.; Noro, M. Three years of study of the Urban Heat Island in Padua: Experimental results. *Sustain. Cities Soc.* **2014**, *10*, 251–258. [CrossRef]
17. Rajagopalan, P.; Lim, K.C.; Jamei, E. Urban heat island and wind flow characteristics of a tropical city. *Sol. Energy* **2014**, *107*, 159–170. [CrossRef]
18. Peng, S.; Feng, Z.; Liao, H.; Huang, B.; Peng, S.; Zhou, T. Spatial-temporal pattern of, and driving forces for, urban heat island in China. *Ecol. Indic.* **2019**, *96*, 127–132. [CrossRef]

19.　Taiwan Central Weather Bureau.　Available online: https://www.cwb.gov.tw/eng/ (accessed on 1 October 2018).

20.　Sailor, D.J. A review of methods for estimating anthropogenic heat and moisture emissions in the urban environment. *Int. J. Climatol.* **2011**, *31*, 189–199. [CrossRef]

21.　Oke, T.R.; Mills, G.; Christen, A.; Voogt, J.A. Introduction. In *Urban Climates*; Cambridge University Press: Cambridge, UK, 2017; pp. 1–13. [CrossRef]

22.　Taiwan Government Website Open Information.　Available online: https://data.gov.tw/en (accessed on 1 November 2018).

23.　Urban and Rural Development Branch. Construction and Planning Agency Ministry of the Interior, R.O.C. Available online: http://Nsp.Tcd.Gov.Tw/Ngis/ (accessed on 1 January 2019).

24.　Lin, H.T.; Chen, K.T.; Kuo, H.C. Experimental Analysis on the Urban Heat Island Effect for the Middle Scale Cities in Taiwan. *J. Plan.* **2001**, *28*, 47–64. (In Chinese) [CrossRef]

25.　Chen, K.T. The Analysis of Urban Heat Island Effects of the Middle and Small Scale Cities in Taiwan. Master's Thesis, Department of Architecture, National Cheng Kung University, Tainan, Taiwan, 2000. Available online: https://hdl.handle.net/11296/gr9mt8 (accessed on 1 March 2019). (In Chinese).

26.　Hsu, H.H. *Climate Change in Taiwan: Scientific Report I 2017 (Summary)*; National Science Council: Taipei, Taiwan, 2017; p. 52. Available online: https://tccip.ncdr.nat.gov.tw/publish_01_one.aspx?bid=20171220135820 (accessed on 1 November 2019). (In Chinese)